Turbulent Transport Reduction and Randomization of Coherent Fluctuations by Zonal Flows in Toroidal Plasma

M. G. Shats,* W. M. Solomon,† and H. Xia

Plasma Research Laboratory, Research School of Physical Sciences and Engineering, Australian National University, Canberra ACT 0200, Australia

(Received 17 September 2002; published 28 March 2003)

Fluctuation-driven particle flux is greatly reduced in the plasma radial region where zonal flows are present in the H-1 toroidal heliac. This occurs without reduction in the fluctuation level. Statistical properties of fluctuations are significantly modified in this region. It is shown that the randomization of phases of coherent structures by zonal flows is responsible for the observed effect. This mechanism of transport reduction complements theoretically predicted random shearing of turbulence by zonal flows and does not require the fluctuations suppression.

DOI: 10.1103/PhysRevLett.90.125002 PACS numbers: 52.35.Ra, 52.35.Mw, 52.55.Hc

Interaction between flows and turbulent structures is the central point of the turbulence self-regulation concept that is being developed with regard to the magnetized plasmas. Both mean (time average) and the time-varying shear flows can be generated by turbulence and both can affect their parent waves and modify the turbulent transport [1]. Time-varying shear flows, or zonal flows (ZF), are nonlinearly generated by turbulence via the inverse cascade mechanism [2]. ZF affect their parent fluctuations [3] and the turbulent-driven fluxes [4] through the mechanism of random shearing [5,6]. The small-scale region of the turbulence spectrum is modified by ZF since both the generation of ZF (inverse cascade) and the shearing leading to the generation of smaller radial scales in turbulence (forward cascade) occur due to the three-wave interactions [4]. The simulation results also indicate that ZF affect both the levels and the structure of the turbulent transport [7–9].

The effect of ZF on large-scale structures is of no less importance since if large turbulent structures are present in the plasma their contribution to the fluctuation-driven particle fluxes exceeds those driven by the small-scale turbulence (see, e.g., [10]). This is the case, for example, in the plasma turbulence described by the Hasegawa-Mima equation [11].

In this Letter we present the first experimental results showing that ZF greatly reduce turbulent fluxes and also change statistical properties of coherent fluctuations through the randomization of their phases. This transport reduction occurs without the reduction in the fluctuations amplitude. It is shown that the randomization in the phases of the coherent structures occurs through their stochastic Doppler shifts in the presence of ZF. These results are very important for understanding the mechanism through which ZF affect the turbulent transport. They can also be useful as the indirect diagnostic of the localization of zonal flows based on the statistical properties of turbulence.

Recently we have reported the first observation of the ZF in the low temperature plasma of the H-1 heliac [12,13], a three-field period helical axis stellarator which has a major radius of $R = 1$ m and a mean minor radius of about $\langle a \rangle \approx 0.2$ m [14]. Experiments described in [12,13] and also in this paper were performed in the plasma produced by ~60 kW of radio-frequency waves at 7 MHz. Plasma parameters are as follows: $n \approx 1 \times 10^{18}$ m^{-3}, $B_T \leq 0.1$ T, $T_e \sim 10$ eV, $T_i \sim 40$ eV in argon at filling pressures of $\sim 3 \times 10^{-5}$ Torr. Various combinations of triple probes are used to characterize plasma parameters. Triple probes provide measurements of the ion saturation current I_s, electron temperature T_e, and the plasma potential ϕ_p. The poloidal electric field is estimated from two poloidally separated triple probes as $E_\theta = (\phi_{p2} - \phi_{p1})/\Delta y$. Simultaneously, we measure the radial electric field using two triple probes, which are separated radially: $E_r = (\phi_{r2} - \phi_{r1})/\Delta r$. More details on the probe geometry can be found in [13].

ZF having $k_r \gg k_\theta \approx 0$ (where k_r and k_θ are the radial and poloidal wave numbers of fluctuations) have been observed in the so-called low confinement mode (L-mode) plasma [12]. These low-frequency ($f_{\mathrm{ZF}} =$ 2–6 kHz) potential structures are generated nonlinearly from the broadband turbulence via three-wave interactions in the inverse cascade process [15].

ZF are not the only structures that are present in the spectrum of the plasma electrostatic potential in L-mode. Strong coherent features with $k_\theta \approx k_r \neq 0$, also generated nonlinearly by the broadband turbulence [15], produce a substantial particle flux which affects the plasma confinement [16]. Radial profiles of the electron density and its fluctuations are shown in Fig. 1(a). Profiles of the fluctuation-driven flux, $\Gamma_{\mathrm{fl}} = \langle \tilde{n}\tilde{V}_r \rangle = \langle \tilde{n}\tilde{E}_\theta \rangle / B_t$ (B_t is the toroidal magnetic field), and of the relative level of the fluctuations in the radial electric field due to the zonal flow at $f = 6$ kHz, $\mathrm{rms}[\tilde{E}_r(f = 6kHz)]/\langle E_r \rangle$, are shown in Fig. 1(b). A remarkable correlation between the

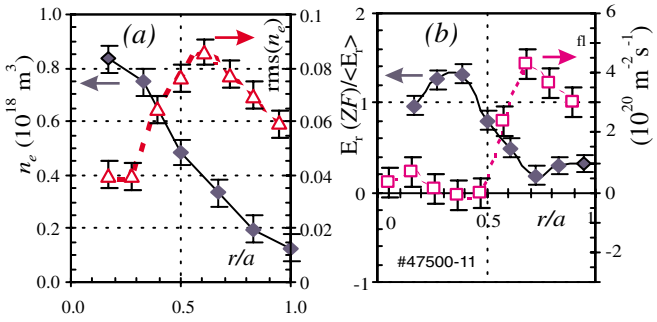

FIG. 1 (color online). Radial profiles of (a) the electron density and the root-mean-square level of its fluctuations and (b) the normalized level of the ZF-driven fluctuations in the radial electric field, rms$[\tilde{E}_r(f = 6\ \mathrm{kHz})]/\langle E_r\rangle$, and of the fluctuation-driven particle flux $\Gamma_{\mathrm{fl}} = \langle \tilde{n}\tilde{E}_\theta\rangle/B_t$.

maximum in the zonal flow and the minimum in Γ_{fl} seen in Fig. 1(b) is amplified by the fact that the reduction in Γ_{fl} is not due to the reduction in the fluctuation level but rather due to the reduced correlation between $\tilde{n}_e$ and $\tilde{E}_\theta$. The structure of the time-resolved fluxes is illustrated in Fig. 2 for two radial positions of Fig. 1 corresponding to the minimum and the maximum of ZF. While in the absence of ZF, at $r/a = 0.68$ [Fig. 2(a)], the flux is dominated by the positive (outward) bursts, and at the ZF maximum positive and negative bursts nearly balance each other resulting in the zero flux [Fig. 2(b)].

Statistical properties of $\tilde{n}_e$ and $\tilde{E}_\theta$ also change in the presence of zonal flows. Figure 3(a) shows radial profiles of kurtosis and skewness of the poloidal electric field fluctuations $\tilde{E}_\theta$. Both are substantially reduced in the radial region of $r/a = (0.2$–$0.5)$. Note that for Gaussian signals $S = K = 0$, so that the observed reduction in both S and K is indicative of the Gaussian statistics of the poloidal electric field fluctuations. Indeed, the probability distribution functions (PDF) of $\tilde{E}_\theta$ at $r/a = 0.37$ has a good Gaussian fit over 3 orders of magnitude as shown in Fig. 3(c), while the PDF at $r/a = 0.68$ is strongly non-Gaussian [Fig. 3(b)].

Frequency spectra of the fluctuations in the floating potential, $\tilde{V}_{\mathrm{fl}}$, poloidal electric field, $\tilde{E}_\theta$, and its phase are shown in Fig. 4. Considering that several strong coherent

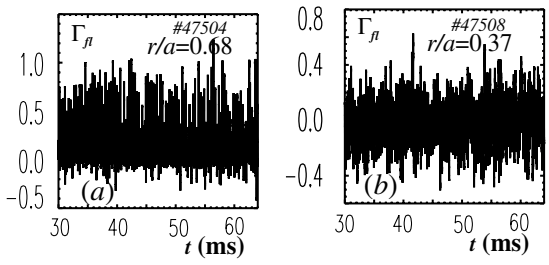

FIG. 2. Time-resolved Γ_{fl} measured in the radial regions corresponding to the (a) minimum and (b) maximum of the ZF level at $r/a = 0.68$ and at $r/a = 0.37$ correspondingly.

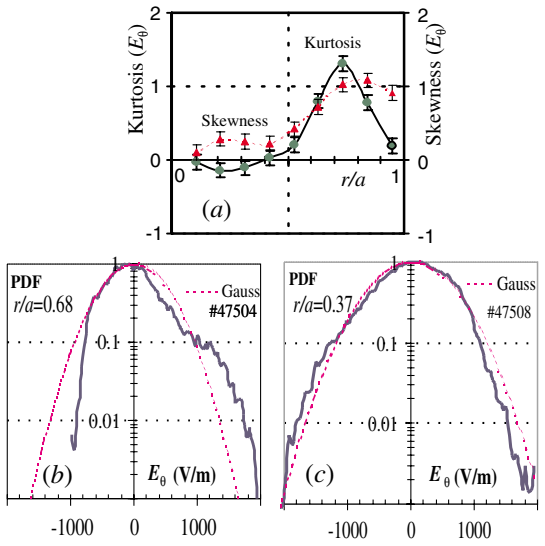

FIG. 3 (color online). (a) Radial profile of kurtosis and skewness of the fluctuations in the poloidal electric field; (b) and (c) are the PDFs of $\tilde{E}_\theta$ measured at $r/a = 0.68$ and at $r/a = 0.37$ correspondingly.

features dominate the spectra, it is natural to expect strongly non-Gaussian statistics of these fluctuations. Zonal flow is present in the spectra of Figs. 4(d)–4(f). It can be identified as a strong feature in the spectrum of the potential fluctuations, $\tilde{V}_{\mathrm{fl}}$, which is not present in the spectrum of the poloidal electric field, $\tilde{E}_\theta$, since ZF has $k_\theta \approx 0$. By comparing frequency spectra in Figs. 4(a)–4(c) (weak zonal flow at $r/a = 0.68$) and Figs. 4(d)–4(f) (maximum of the zonal flow at $r/a = 0.37$) we observe that phases of strongest harmonics of $\tilde{E}_\theta$ become random in the presence of the zonal flow. The spectra in Fig. 4

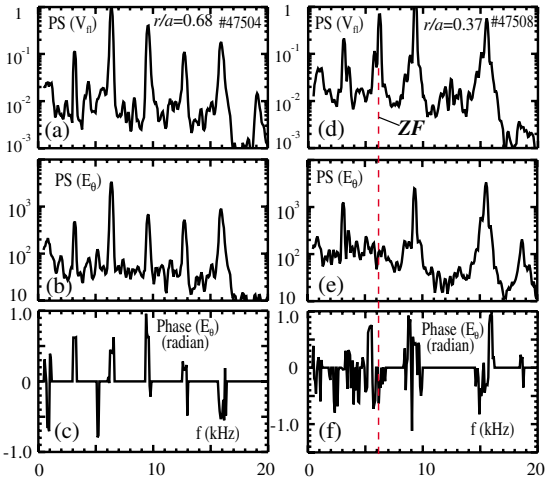

FIG. 4 (color online). Frequency power spectra (PS) of the fluctuations in the poloidal electric field $\tilde{E}_\theta$ and of the phase of $\tilde{E}_\theta$ measured at the (a)–(c) minimum and at the (d)–(f) maximum of ZF at $r/a = 0.68$ and at $r/a = 0.37$ correspondingly.

have been computed for the 32 ms long time samples of signals. The samples are split into four overlapping time segments, and the computed frequency spectra are then averaged over four points. Such statistical averaging of the spectral estimation of the fluctuation phases leads to different results in the presence of ZF [Fig. 4(f)] and without it [Fig. 4(c)]. While in the absence of ZF phases are well-defined and the statistical averaging leads to a fast convergence of the spectral estimation to some finite (though physically irrelevant) value [Fig. 4(c)], at the ZF maximum phases are statistically independent in different realizations, their average is randomly distributed, and it does not converge as fast to a finite value. This statistically unstable spectral estimation of the fluctuation phase is indicative of the phase randomization. The randomization of phases of the $\tilde{E}_\theta$ harmonics, similar to that seen in Fig. 4(f) is observed only in the presence of zonal flows. Note also that the spectral broadening of the features at the ZF maximum [Figs. 4(d) and 4(e)] is noticeably increased.

The level of the three-wave interactions in the spectra exhibiting turbulent structures (including ZF) has been shown to be high in our conditions [12]. It is well-known that the characteristic nonlinear interaction time and the level of the three-wave interactions depend on whether phases of the interacting waves are coherent or random [17]. The transition from the coherent phase approximation to the random phase limit coincides with the spectral broadening of the wave packets and with the reduction in the coherence of the participating waves [17].

The phase randomization of the coherent spectral features in the presence of ZF in our experiment indeed leads to a reduced phase coupling between these modes. A quantity that characterizes a degree of phase coupling in the spectrum is the autobicoherence, or normalized bispectrum [18] defined as $b_f^2(f_1, f_2) = B(f_1, f_2)^2/[\langle|E_{\theta f1}E_{\theta f2}|^2\rangle P(f)]$, where $B(f_1, f_2) = \langle E_{\theta f1}E_{\theta f2}E^*_{\theta f}\rangle$ is the autobispectrum and $P(f)$ is the autopower spectrum. We also compute the summed bicoherence, $\mathrm{SB}(f) = \sum_{f=f_1+f_2} b_f^2(f_1, f_2)$. This quantity gives a measure of the total phase coupling to the frequency f from all frequencies f_1 and f_2 in the spectrum satisfying $f = f_1 + f_2$.

Figure 5 shows the frequency spectrum of the summed autobicoherence for spectra of Fig. 4. Here the threshold for the SB computation is set to include contributions to the bispectrum from the spectral components whose amplitudes are greater than 10^{-2} of the maximum of the spectrum. Thus we estimate only the phase coupling between strongest harmonics and exclude contributions from the three-wave interactions in the broadband part of the turbulence spectrum. From Fig. 5(a) we observe that in the presence of ZF the SB is reduced for most of the spectral features by a factor of at least 2. When the contribution to the bispectrum from the broadband turbulence is included by thresholding computations to the

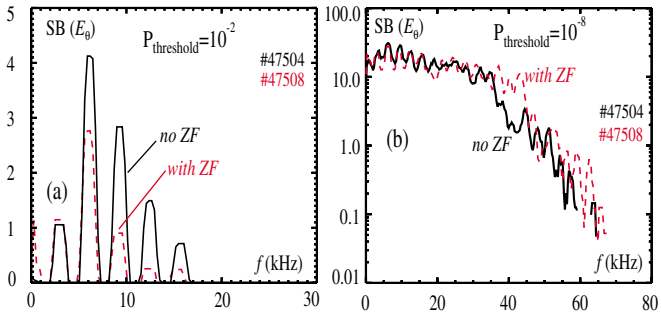

FIG. 5 (color online). Summed autobicoherence of $\tilde{E}_\theta$ computed for signals measured at $r/a = 0.68$ (solid) and at $r/a = 0.37$ (dotted) for two thresholds in the spectral power density: (a) $P_{\mathrm{threshold}} = 10^{-2}$ and (b) $P_{\mathrm{threshold}} = 10^{-8}$.

level of 10^{-8} of the maximum of the spectrum, no reduction in the summed autobicoherence is observed [Fig. 5(b)]. This seems to be natural because waves with random phases dominate three-wave interactions in the broadband part of the spectrum.

We model the spectrum of the coherent fluctuations in the form

$$Y = \sum_{i=1}^{5} A_i \sin[\omega_i + \omega_i^{\mathrm{rand}}(t)]t + \mathrm{noise}, \qquad (1)$$

where we introduce a small random correction ω^{rand} to the phase of each of the coherent harmonics. Here ω_i^{rand} changes randomly in the range between $\pm\omega_i^{\mathrm{rand}}$. The statistical moments and the total summed bicoherence ($= \sum_f \mathrm{SB}(f)$) are computed for the model signal of Eq. (1). Kurtosis and skewness are shown in Fig. 6(a) versus the degree of randomization defined as $\mathrm{DR} = \omega_i^{\mathrm{rand}}/\omega_i$. The noise level was zero in these calculations. At $\mathrm{DR} \approx 0.1$ the skewness of the signal is substantially reduced, while kurtosis becomes negative as seen in Fig. 6. The total summed bicoherence of the signal [Fig. 6(b)] is reduced at $\mathrm{DR} \approx 0.1$ by almost 2 orders of magnitude. The addition of the random noise to the signal of Eq. (1) does not change the moments and the

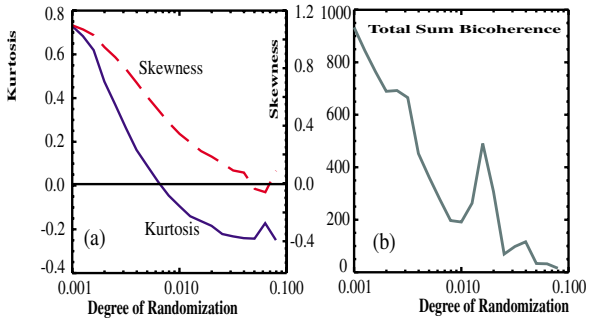

FIG. 6 (color online). (a) Kurtosis and skewness of the model signals of Eq. (1) and (b) the total summed autobicoherence versus the degree of the phase randomization.

bicoherence as much, even when the signal is below the noise. This elementary model qualitatively reproduces basic observations of Figs. 3 and 5.

The reported results can be interpreted as follows. The velocity of the poloidally propagating coherent structures is Doppler shifted by the lower-frequency zonal flow as

$$E_{\theta k} \sin\left[\left(\omega_k + k_\theta \frac{\tilde{E}_r(\Omega)}{B_t}\right)t\right], \tag{2}$$

where Ω is the frequency of the zonal flow seen as the time-varying radial electric field. If this Doppler shift introduces some randomization in the phase of the propagating potential structure, this would be equivalent to the introduction of the random phase correction ω^{rand} in Eq. (1), affecting both higher- and lower-frequency modes. The degree of randomization by ZF can be estimated from the broadening of the zonal flow spectrum as $[k_\theta \tilde{E}_r(\Omega)/B_t] \cdot (\Delta\Omega/\Omega)$, where $\Delta\Omega/\Omega \approx 0.1$ as seen in Fig. 4(d). For the experimentally measured parameters ($\sqrt{\langle \tilde{E}_r^2 \rangle} = 200$ V/m, $B_t = 0.06$ T, $k_\theta = 40$ m^{-1}, $\omega_k = 10^5$ s^{-1}) we estimate that this noncoherence in the zonal flow is equivalent to the degree of randomization of DR $= 0.1$.

The fluctuation-driven particle flux is defined in the frequency domain as [19]

$$\Gamma_{\text{fl}} = \frac{2}{B}\int_0^\infty d\omega [P_n P_E]^{1/2} |\gamma_{nE}| \cos[\alpha_{nE}], \tag{3}$$

where $0 \le |\gamma_{nE}| \le 1$ and α_{nE} are the coherence and the phase shift between $\tilde{n}_e$ and $\tilde{E}_\theta$ correspondingly and P_n and P_E are the spectral densities of the fluctuations. Equation (3) shows that the particle flux can be reduced by suppressing the turbulence (P_n and P_E reduction), by decorrelating density and potential fluctuations ($\gamma_{nE} \to 0$), or by changing the relative phase α_{nE} between them. The phase randomization in either $\tilde{n}_e$ and $\tilde{E}_\theta$ or both should result in the decrease of the time-average coherence, γ_{nE}, between these fluctuations and may also change the cross phase, α_{nE}. This would affect the fluctuation-driven particle flux without suppressing the fluctuations, as it has been observed in the reported experiments.

To summarize, we have observed a strong reduction in the fluctuation-driven particle flux in the presence of zonal flows. Zonal flows have been shown to change statistical properties of the fluctuations due to the randomization of phases of coherent structures dominating spectra. These observations are qualitatively consistent with the model of the random Doppler shift of the turbulent structures by zonal flows.

One of the authors (M. S.) thanks P. H. Diamond and M. A. Malkov for useful discussions of the results.

*Electronic address: michael.shats@anu.edu.au
†Current address: Princeton University, Plasma Physics Laboratory, P.O. Box 451, Princeton, NJ 08543.

[1] P. W. Terry, Rev. Mod. Phys. **72**, 109 (2000).
[2] A. Hasegawa and M. Wakatani, Phys. Rev. Lett. **59**, 1581 (1987).
[3] P. H. Diamond *et al.*, in *Plasma Physics and Controlled Nuclear Fusion Research, Proceedings of the 17th IAEA Fusion Energy Conference, Yokohama, Japan, 1998* (International Atomics Energy Agency, Vienna, 1998), p. IAEA-CN-69/ TH3/1.
[4] M. A. Malkov *et al.*, Phys. Plasmas **8**, 5073 (2001).
[5] H. Biglari, P. H. Diamond, and P. W. Terry, Phys. Fluids B **2**, 1 (1990).
[6] T. S. Hahm *et al.*, Phys. Plasmas **6**, 922 (1999).
[7] Z. Lin *et al.*, Science **281**, 1835 (1998).
[8] K. Hallatschek and D. Biskamp, Phys. Rev. Lett. **86**, 1223 (2001).
[9] S. Benkadda *et al.*, Nucl. Fusion **41**, 995 (2001).
[10] W. Horton and Y. H. Ychikawa, *Chaos and Structures in Nonlinear Plasmas* (World Scientific, Singapore, 1996).
[11] A. Hasegawa and K. Mima, Phys. Fluids **21**, 87 (1978).
[12] M. G. Shats and W. M. Solomon, Phys. Rev. Lett. **88**, 045001 (2002).
[13] M. G. Shats and W. M. Solomon, New J. Phys. **4**, 30 (2002).
[14] S. M. Hamberger *et al.*, Fusion Technol. **17**, 123 (1990).
[15] H. Xia and M. G. Shats (to be published).
[16] M. G. Shats, Plasma Phys. Controlled Fusion **41**, 1357 (1999).
[17] V. N. Tsytovich, *Nonlinear Effects in Plasma* (Plenum, New York, 1970).
[18] Y. C. Kim and E. J. Powers, IEEE Trans. Plasma Sci. **PS-7**, 120 (1979).
[19] E. J. Powers, Nucl. Fusion **14**, 749 (1974).